COMPDYN 2013
4th ECCOMAS Thematic Conference on
Computational Methods in Structural Dynamics and Earthquake Engineering
M. Papadrakakis, V. Papadopoulos, V. Plevris (eds.)
Kos Island, Greece, 12–14 June 2013

OPTIMAL CONTROL DESIGN BY ADJOINT-BASED OPTIMIZATION FOR ACTIVE MASS DAMPER WITH DRY FRICTION

Domenico Guida[1], **Fabio Nilvetti**[1], **and Carmine M. Pappalardo**[1]

[1]University of Salerno
via Ponte don Melillo - 84084 - Fisciano (SA) - Italy
e-mail: {guida,fnilvetti,cpappalardo}@unisa.it

Keywords: Optimal Control, Adjoint-Based Optimization, Active Mass Damper, Dry Friction.

Abstract. *The goal of our research is to set up an effective procedure to design control laws of Hybrid Mass Dampers (HMDs) in order to mitigate structural vibration. The system under test is a two-storey frame equipped with an active vibration absorber located on the top of it. The vibration absorber is subjected to dry friction and is driven by a control force. The two-storey frame is subjected to a base excitation whose harmonic content is close to the system natural frequencies. The control actuator is located between the second floor and the mass damper. The control law is obtained using optimal control theory and is calculated solving a constrained minimization problem. The cost function penalizes the control effort and the state deviation from a reference position. Since the system model is non-linear, the optimal control problem is to be solved numerically. The numerical algorithm used in the proposed procedure is an iterative adjoint-based optimization method. This method combines the non-linear conjugate gradient algorithm with adjoint-based gradient computation.*

In this paper authors propose an analytical model of the dry friction force which describes the interaction between the absorber and structure. Simulations show that the designed control law significantly reduces the structural vibration caused by the base excitation.

1 INTRODUCTION

Dynamic Vibration Absorbers (DVAs) or Tuned Mass Dampers (TMDs) are mechanical devices capable of reducing potentially dangerous vibrations of structural systems [1]. The basic configuration of DVAs comprises inertia, stiffness and damping elements which can be properly designed to absorb the vibratory energy of the mechanical system to be protected. Since DVAs operate without using an external energy supply, they are passive control systems. On the other hand, Active Control Systems (ACSs) are electro-mechanical devices which can modify the motion of the structure to be protected through the action of external forces [2]. The fundamental scheme for ACSs consists of four parts: 1) the mechanical system to be preserved, 2) sensors located on the system to measure structural vibrations and external excitations, 3) a control unit necessary to process the measured information, to compute the control actions according to a dedicated control algorithm and to drive the actuators, 4) actuators necessary to provide the required forces. Active Vibration Absorbers (AVAs) or Hybrid Mass Dampers (HMDs) are a natural evolution of DVAs, TMDs and ACSs [3]. They combine the advantages of passive vibration absorbers with the versatility of active controllers. AVAs or HMDs are designed to work as DVAs or TMDs but are subjected to control forces delivered by control actuators. The performances of AVAs or HMDs can be considerably improved introducing dry friction dampers in the system [4]. The dynamic properties of vibration absorbers subjected to dry friction forces significantly differ from those of linear viscous absorbers. Indeed, the introduction of dry friction dampers complicates the system model, which becomes nonlinear, and therefore the control actions cannot be computed using classical control algorithm. In this paper authors propose the development of a new control scheme for a two-storey system equipped with a vibration absorber subjected to a dry friction force.

2 SYSTEM MODEL

2.1 System Description

The system being analysed is showed in figure 1. All system data are reported in table 1.

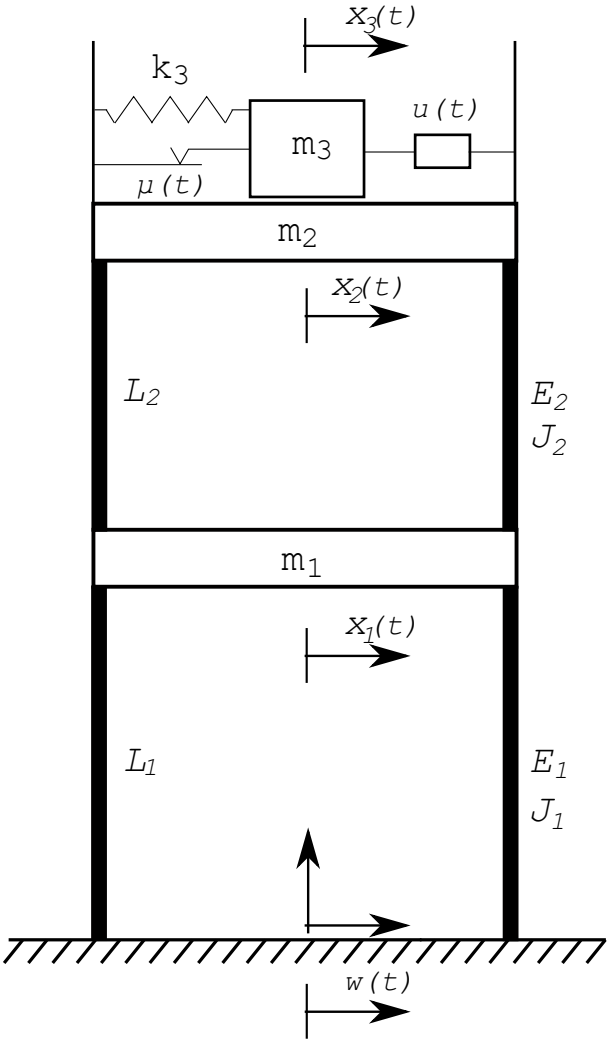

Figure 1: Two-Storey Building with Controlled Friction Absorber

The system is essentially a two-storey building with an absorber located on the second floor [5], [6]. The frequency range of interest encompasses frequencies below $15[Hz]$. The two-storey frame is modelled as a two degrees of freedom system. The system floors were modelled as bulky elements with mass m_1 and m_2. The supporting beams are of length L_1 and L_2 with a second moment of area equal to J_1 and J_2 and are made of steel with elastic modulus E_1 and E_2. The flexible elements provide the stiffness k_1 and k_2 which can be computed assuming a clamped-clamped beam configuration. The system natural frequencies are respectively equal to $f_{n,1} = 3.23[Hz]$ and $f_{n,2} = 6.82[Hz]$. The two-storey frame is subjected to proportional damping with coefficients α and β [7]. The absorber is located on the second floor, has a mass m_3 and is connected to the second floor with a spring of stiffness k_3. The absorber can slide on

the second floor and is subjected to a dry friction force with a friction coefficient μ_0. Friction force was smoothed to facilitate the computation [8] according to two different models: $\eta_1(t)$ for Coulomb friction and $\eta_2(t)$ for Stribeck friction. The first approximated friction model can be written as follows:

$$\mu(t) = \mu_0 \eta_1(t) = \mu_0 D_1 \left(1 - \frac{2}{e^{2D_2(\dot{x}_3(t) - \dot{x}_2(t))} + 1}\right) \tag{1}$$

where μ_0 is the dry friction coefficient and $\eta_1(t)$ is the function which approximates the Coulomb friction model. The friction model (1) is showed in figure 2. This is a smoothed

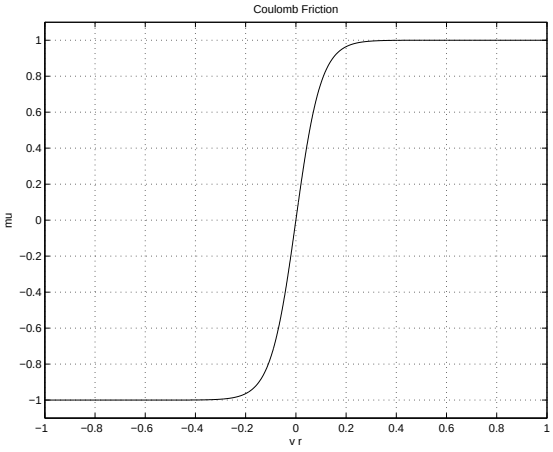

Figure 2: $\eta_1(t)$ - Approximated Friction Model 1

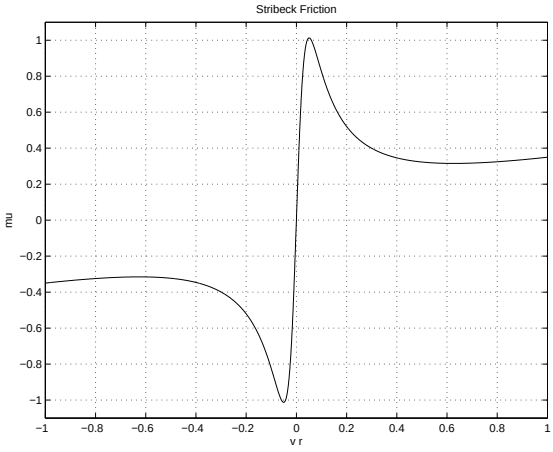

Figure 3: $\eta_2(t)$ - Approximated Friction Model 2

version of the Coulomb friction model which approaches the discontinuous model when the parameter D_2 tends to infinity. The second approximated friction model can be written as follows:

$$\mu(t) = \mu_0 \eta_2(t) = \mu_0 \left(\frac{C_1(\dot{x}_3(t) - \dot{x}_2(t))}{C_2 + C_3(\dot{x}_3(t) - \dot{x}_2(t))^2} + C_4(\dot{x}_3(t) - \dot{x}_2(t))\right) \tag{2}$$

where μ_0 is the dry friction coefficient and $\eta_2(t)$ is the function which approximates the Stribeck friction model. The friction model (2) is showed in figure 3. This smoothed version of the dry friction model approaches the discontinuous model when the parameter C_3 tends to infinity. On the other hand, the control actuator is interposed between the absorber and the second floor. The whole system is excited by a ground motion $w(t)$. Considering a worst-case scenario, the ground motion $w(t)$ is assumed as a superposition of two harmonic displacements whose excitation frequencies are close to the two-storey frame natural frequencies. Indeed:

$$w(t) = W_1 \sin(2\pi f_1 t) + W_2 \sin(2\pi f_2 t) \tag{3}$$

where W_1 and W_2 are the ground motion amplitudes whereas f_1 and f_2 are the ground motion excitation frequencies.

2.2 Equations of Motion

The configuration of the system can be described by a set of $n_2 = 3$ generalised coordinates which can be grouped into a vector $q(t)$ as:

$$q(t) = \begin{bmatrix} x_1(t) \\ x_2(t) \\ x_3(t) \end{bmatrix} \tag{4}$$

The Lagrangian coordinates $x_1(t)$ and $x_2(t)$ represent the displacements of each floor whereas the Lagrangian coordinate $x_3(t)$ represent the displacement of the absorber. The system model encompasses three degrees of freedom and is non-linear because of the dry friction force. In general, the matrix form of a non-linear dynamic system model can be written as follows:

$$M(t)\ddot{q}(t) = Q(t) \tag{5}$$

where $M(t)$ represents system mass matrix and $Q(t)$ denotes the total generalised forces acting on the system. This is a set of $n_2 = 3$ ordinary differential equations which requires a set of $2n_2 = 6$ initial conditions $q(0) = q_0$ and $\dot{q}(0) = p_0$. For the system being analysed, the mass matrix $M(t)$ and the vector of generalised forces $Q(t)$ can be derived using Lagrangian Dynamics to yield:

$$M(t) = \begin{bmatrix} m_1 & 0 & 0 \\ 0 & m_2 & 0 \\ 0 & 0 & m_3 \end{bmatrix} \tag{6}$$

$$Q(t) = \begin{bmatrix} -k_1(x_1(t) - w(t)) - k_2(x_1(t) - x_2(t)) + \\ -r_1(\dot{x}_1(t) - \dot{w}(t)) - r_2(\dot{x}_1(t) - \dot{x}_2(t)) \\ \\ -k_2(x_2(t) - x_1(t)) - k_3(x_2(t) - x_3(t)) + \\ -r_2(\dot{x}_2(t) - \dot{x}_1(t)) - r_3(\dot{x}_2(t) - \dot{x}_3(t)) + m_3 g\mu(t) \\ \\ -k_3(x_3(t) - x_2(t)) - m_3 g\mu(t) \end{bmatrix} \tag{7}$$

If a control action $Q_c(t)$ is introduced on the system, the matrix form of system equations of motion becomes:

$$M(t)\ddot{q}(t) = Q(t) + Q_c(t) \tag{8}$$

In the case of the system under test, the control action is interposed between the second floor and the mass damper:

$$Q_c(t) = B_2(t)u(t) \tag{9}$$

where $u(t)$ is the control input and $B_2(t)$ is a Boolean matrix defined as follows:

$$B_2(t) = \begin{bmatrix} -1 \\ 1 \end{bmatrix} \tag{10}$$

System equations of motion can be used as an analytical model to design a controller whose objective is to reduce structural vibration.

2.3 State-Space Model

The preliminary step to design a control system consists in rewriting system equations of motion (8) in the state-space form. The system state can be represented using a state vector of dimension $n = 2n_2 = 6$ defined as:

$$z(t) = \begin{bmatrix} q(t) \\ \dot{q}(t) \end{bmatrix} \tag{11}$$

The system equations of motion (8) can be rewritten in term of the state vector as follows:

$$\dot{z}(t) = f(t) + B_c(t)u(t) \tag{12}$$

where $f(t)$ is a non-linear state function and $B_c(t)$ is the state influence matrix which can be respectively computed as:

$$f(t) = \begin{bmatrix} \dot{q}(t) \\ M^{-1}(t)Q(t) \end{bmatrix} \tag{13}$$

$$B_c = \begin{bmatrix} O \\ M^{-1}(t)B_2(t) \end{bmatrix} \tag{14}$$

This is the state-space form of system equations of motion namely a set of $n = 2n_2 = 6$ first-order differential equations which constitute the system state-space model. The initial state $z(0) = z_0$ required to solve the state-space equations can be derived from system initial conditions $q(0) = q_0$ and $\dot{q}(0) = p_0$.

3 CONTROL STRATEGY

3.1 Optimal Control

In general, the raison d'etre of a control system is to influence the dynamics of a mechanical system in order to make it behave in a desirable manner. An approach to design a control system is to use optimal control methods. Optimal control consists in implementing mathematical optimization methods for deriving control laws [9]. The essence of optimal control theory can be summarised as follows. The key idea is to find the control action $u(t)$ which minimizes a cost function J_c. The cost function or performance index is a quantitative expression which can be used to determine how well a particular control law meets the design goals. A general cost functional can be written as:

$$J_c = h(T) + \int_0^T g(t)dt \tag{15}$$

where $h(T)$ and $g(t)$ are two analytical functions which, in the case of a quadratic cost index, are defined as follows:

$$h(T) = \frac{1}{2}(z(T) - \bar{z}(T))^T Q_T (z(T) - \bar{z}(T)) \tag{16}$$

$$g(t) = \frac{1}{2}(z(t) - \bar{z}(t))^T Q_z (z(t) - \bar{z}(t)) + \frac{1}{2}(u(t) - \bar{u}(t))^T Q_u (u(t) - \bar{u}(t)) \tag{17}$$

where $\bar{z}(t)$ and $\bar{u}(t)$ are respectively the reference trajectory and the reference control action used in tracking problems whereas Q_T, Q_z and Q_u are positive semi-definite weight matrices. The definition of the weight matrices Q_T, Q_z and Q_u represents a crucial step in the design process which drastically influences the resulting control law. In regulation problems the reference functions $\bar{z}(t)$ and $\bar{u}(t)$ are set equal to zero. The system equations of motion (12) represent a set of dynamic constraints for the minimization problem. An approach to solve this problem consists in employing calculus of variation techniques in order to obtain the necessary conditions which minimize the cost functional [9]. The first step consists in defining the Hamiltonian function as:

$$H_c(t) = g(t) + \lambda^T(t)(f(t) + B_c(t)u(t)) \tag{18}$$

where $\lambda(t)$ is a co-state vector which contains the Lagrange multipliers that arise from adjoining the state-space equations of motion (12) to the cost functional (15). Thus, the resulting optimal conditions can be computed from the Hamiltonian function (18) as follows:

$$\dot{z}(t) = (\frac{\partial H_c(t)}{\partial \lambda(t)})^T = f(t) + B_c(t)u(t) \tag{19}$$

$$\dot{\lambda}(t) = -(\frac{\partial H_c(t)}{\partial z(t)})^T = -Q_z(z(t) - \bar{z}(t)) - A_c^T(t)\lambda(t) \tag{20}$$

Where $A_c(t)$ is a state matrix derived from the linearization of the state function $f(t)$ around the reference functions $\bar{z}(t)$ and $\bar{u}(t)$. The fist set of equations (19) is exactly the state-space form of system equations of motion whereas the second set of equations (20) represents the co-state equations or adjoint equations. The adjoint equations (20) require a set of terminal conditions which can be computed as:

$$\lambda(T) = (\frac{\partial h(T)}{\partial z(T)})^T = Q_T(z(T) - \bar{z}(T)) \tag{21}$$

The resulting equations are necessary to solve the constrained minimization problem and form a two-point boundary-value problem. Indeed, the set of system equations of motion (12) and adjoint equations (20) constitutes a coupled non-linear problem which can be solved numerically by using non-linear optimization techniques.

3.2 Iterative Adjoint-Based Optimization

A method to solve the two-point boundary-value problem (12), (20) resulting from the minimization of the cost function (15) consists in using an iterative adjoint-based optimization approach. The key idea of the iterative adjoint-based optimization method is to exploit the knowledge of the cost functional gradient to solve the minimization problem [10], [11]. Indeed, the gradient of the performance index can be derived from the Hamiltonian function (18) as follows:

$$G_c(t) = (\frac{\partial H_c(t)}{\partial u(t)})^T = Q_u(u(t) - \bar{u}(t)) + B_c^T(t)\lambda(t) \tag{22}$$

The gradient (22) is readily determined once that the adjoint state $\lambda(t)$ is known solving the adjoint equations (20) and it can be used in an iterative gradient-based optimization algorithm in order to gradually improve the approximated solution towards the cost function minimum. Typically, to accomplish this task a line search method is used, such as the steepest descent method or the non-linear conjugate gradient method [12]. Algorithms based on the line search strategy use a descent direction e_k and search the minimum along this direction from the current solution u_k to the next solution u_{k+1} corresponding to a lower cost index. Indeed, using a line search method the control input can be iteratively calculated as:

$$u_{k+1} = u_k + \alpha_k e_k \tag{23}$$

where α_k is a line parameter which represents the step length corresponding to the current iteration. The minimization algorithms based on a line search strategy differ from each other with the selection of the descent direction e_k. The steepest descent method sets the descent direction equal to the cost function gradient:

$$e_k = -G_{c,k} \tag{24}$$

The basic idea is to perform the line search of the minimum along the direction where the cost function decreases the most rapidly. This method can be very slow in some problems because the choice of the descent direction is too rigid. On the other hand, the non-linear conjugate gradient method defines the descent direction as follows:

$$e_k = -G_{c,k} + \beta_k e_{k-1} \tag{25}$$

where β_k is a parameter which ensures that the descent direction e_{k-1} and e_k are conjugate [10], [12]. Three of the best known formulas for β_k are titled Fletcher-Reeves, Polak-Ribiere and Hestenes-Stiefel after their developers [10], [12]. These formulae can be respectively written as follows:

$$\beta_k^{FR} = \frac{G_{c,k}^T G_{c,k}}{G_{c,k-1}^T G_{c,k-1}} \tag{26}$$

$$\beta_k^{PR} = \frac{G_{c,k}^T (G_{c,k} - G_{c,k-1})}{G_{c,k-1}^T G_{c,k-1}} \tag{27}$$

$$\beta_k^{HS} = -\frac{G_{c,k}^T (G_{c,k} - G_{c,k-1})}{e_k^T (G_{c,k} - G_{c,k-1})} \tag{28}$$

where β_k^{FR} is Fletcher-Reeves parameter, β_k^{PR} is Polak-Ribiere parameter and β_k^{HS} is Hestenes-Stiefel parameter. Once that the descent direction has been set, the solution can be found with a minimum search algorithm such as Brent method or golden section method [10], [11]. The overall procedure to implement an iterative adjoint-based optimization of the control action can be summarized as follows:

- Step 1) Select an initial control input u_k;

- Step 2) Use the control input u_k to solve numerically system state equations (12) in order to obtain the system state z_k;

- Step 3) Use the system state z_k to solve numerically adjoint equations (20) in order to obtain the adjoint state λ_k;

- Step 4) Use the control input u_k and the adjoint state λ_k to compute the cost function gradient $G_{c,k}$ by using equations (22);

- Step 5) Use the cost function gradient $G_{c,k}$ to compute the descent direction e_k by using equations (25);

- Step 6) Use the descent direction e_k in order to obtain numerically the line parameter α_k by a line search numerical method;

- Step 7) Use the line parameter α_k to update the control input u_{k+1} by using equations (23);

- Step 8) Restart from step 1 if the chosen stopping criteria is not satisfied;

To solve numerically the state equations and the adjoint state equations Runge-Kutta methods are adequate. To stop the algorithm a tolerance on the cost function variation can be assigned, namely when no progress are made the iteration must stop.

4 RESULTS AND DISCUSSION

4.1 Control Design

A controller was designed using the iterative adjoint-based optimization method described in the preceding section. The penalty matrices were chosen as follows:

$$Q_T = diag(10^4, 10^4, 10^4, 10^4, 10^4, 10^4) \tag{29}$$

$$Q_z = diag(10^4, 10^4, 10^4, 10^4, 10^4, 10^4) \tag{30}$$

$$Q_u = 10^{-4} \tag{31}$$

The weight matrices Q_T and Q_z drastically penalise the displacements and the velocities of each system floor and of the absorber. On the other hand, the control effort is relatively less penalised by the weight matrix Q_u. Two different case study has been analysed and two different control law has been designed. The two case study differ for the friction model utilised. In the first case study the friction model utilised is a smoothed version of Coulomb friction (1) whose model is showed in figure 2 whereas in the second case study the friction model utilised is a smoothed version of Stribeck friction (2) whose model is showed in figure 3.

4.2 Case Study 1

In this case study the friction model (1) was used. First the system motion without the controller has been analysed. The displacements of system floors in the case of the uncontrolled motion are represented in figure 4 and 6 whereas the displacements of system floors in the case of the controlled motion are represented in figure 5 and 7. The displacement of the absorber in

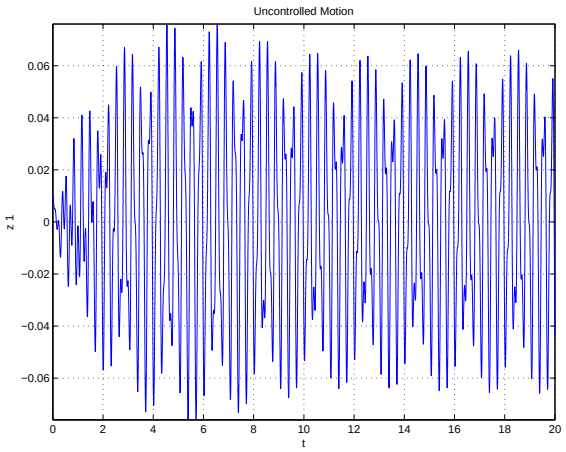

Figure 4: $x_1(t)$ - Uncontrolled Motion - Case Study 1

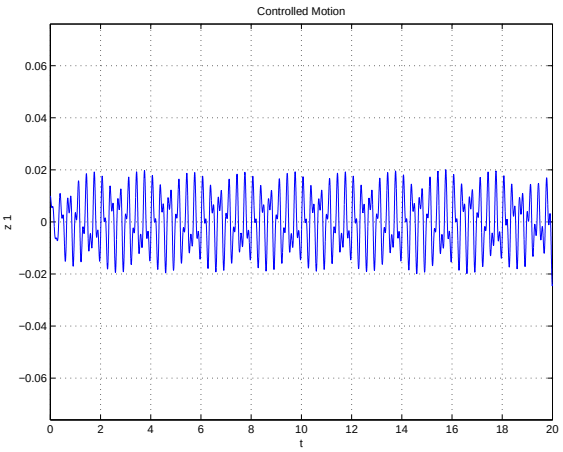

Figure 5: $x_1(t)$ - Controlled Motion - Case Study 1

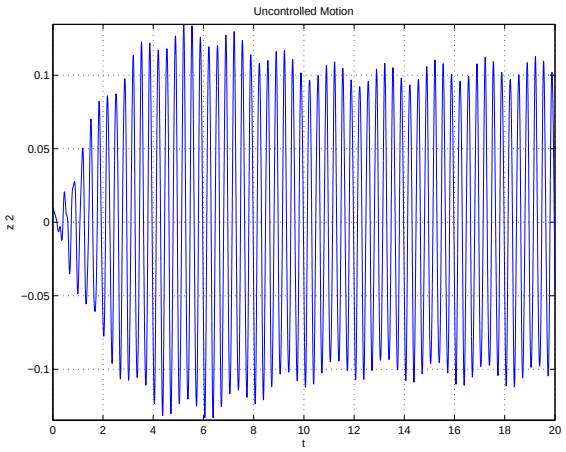

Figure 6: $x_2(t)$ - Uncontrolled Motion - Case Study 1

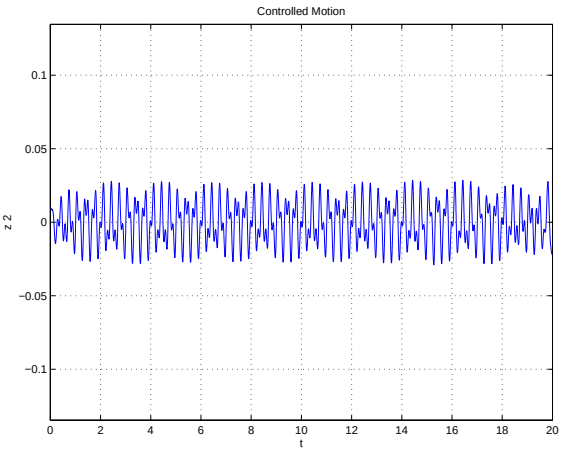

Figure 7: $x_2(t)$ - Controlled Motion - Case Study 1

the case of the uncontrolled motion is represented in figure 8 whereas the displacement of the absorber in the case of the controlled motion is represented in figure 9. The velocities of system floors and of the absorber in the case of the controlled motion exhibit an amplitude reduction qualitatively similar to that of their respective displacements. The iterative decrease of the cost function is represented in figure 10. The resulting controller is represented in figure 11. As can be seen from the preceding figures, the introduction of the controller drastically reduces the magnitudes of system displacements and velocities. This reduction can be quantified comparing the maximum amplitudes of system motion with and without the controller. Indeed:

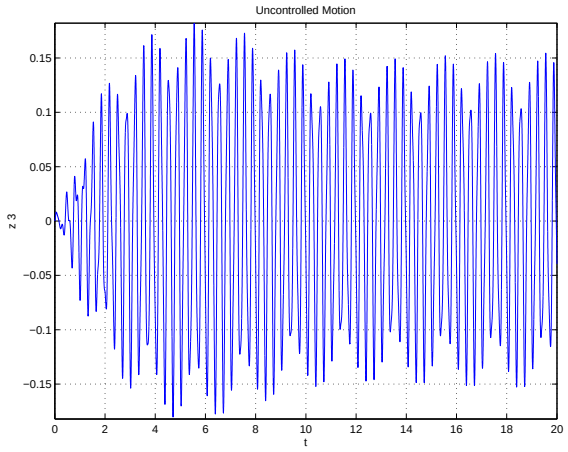

Figure 8: $x_3(t)$ - Uncontrolled Motion - Case Study 1

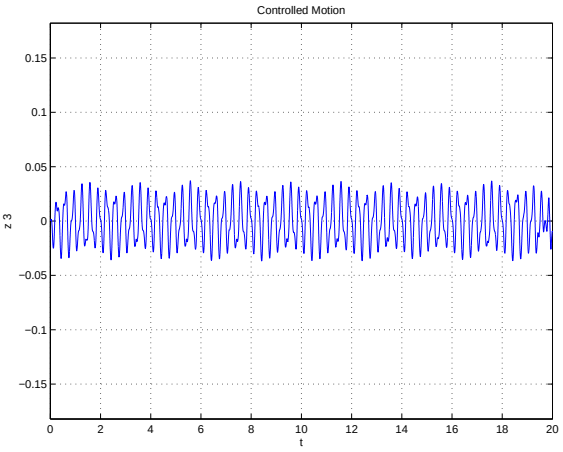

Figure 9: $x_3(t)$ - Controlled Motion - Case Study 1

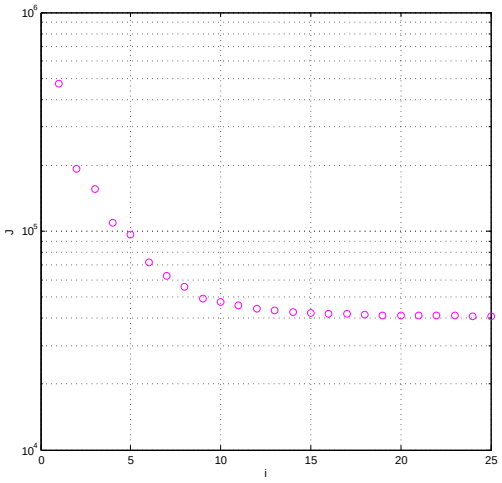

Figure 10: J_c - Performance Index - Case Study 1

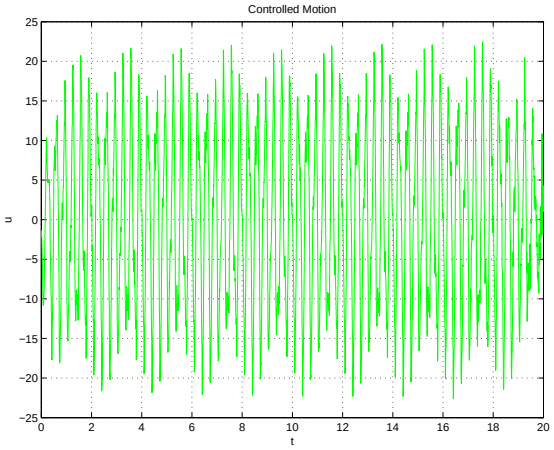

Figure 11: $u(t)$ - Control Action - Case Study 1

$$\varepsilon_{r,x_i} = \frac{\max\limits_{t\in[0,T]}(\mathrm{abs}(x_{i,uncontrolled}(t))) - \max\limits_{t\in[0,T]}(\mathrm{abs}(x_{i,controlled}(t)))}{\max\limits_{t\in[0,T]}(\mathrm{abs}(x_{i,uncontrolled}(t)))} = \begin{cases} 0.6770 \\ 0.7852 \\ 0.7968 \end{cases} \tag{32}$$

$$\varepsilon_{r,\dot{x}_i} = \frac{\max\limits_{t\in[0,T]}(\mathrm{abs}(\dot{x}_{i,uncontrolled}(t))) - \max\limits_{t\in[0,T]}(\mathrm{abs}(\dot{x}_{i,controlled}(t)))}{\max\limits_{t\in[0,T]}(\mathrm{abs}(\dot{x}_{i,uncontrolled}(t)))} = \begin{cases} 0.7081 \\ 0.7090 \\ 0.7495 \end{cases} \tag{33}$$

The magnitude reductions of floors and absorber displacements are greater than the 67% whereas the magnitude reductions of floors and absorber velocities are greater than the 70%.

4.3 Case Study 2

In this case study the friction model (2) was used. First the system motion without the controller has been analysed. The displacements of system floors in the case of the uncontrolled motion are represented in figure 12 and 14 whereas the displacements of system floors in the case of the controlled motion are represented in figure 13 and 15. The displacement of the

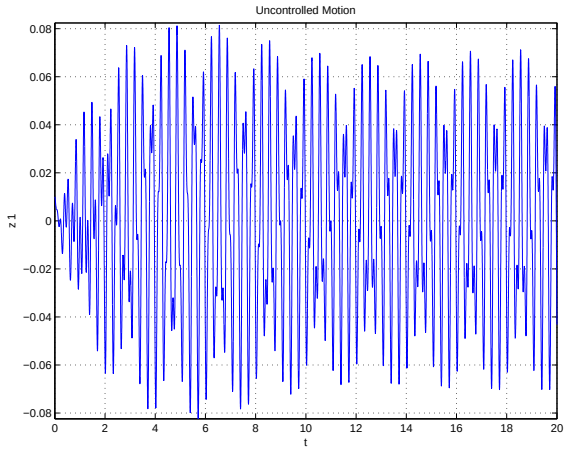

Figure 12: $x_1(t)$ - Uncontrolled Motion - Case Study 2

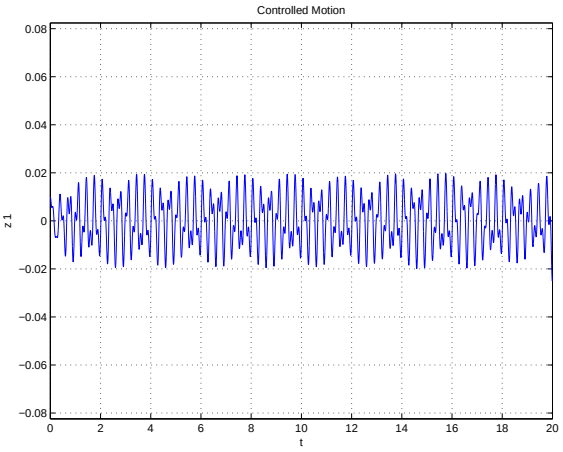

Figure 13: $x_1(t)$ - Controlled Motion - Case Study 2

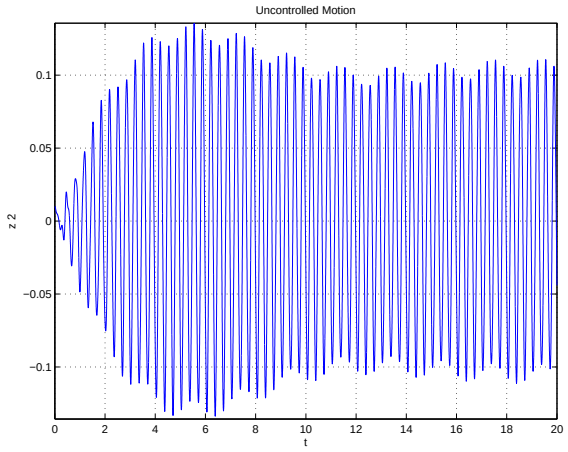

Figure 14: $x_2(t)$ - Uncontrolled Motion - Case Study 2

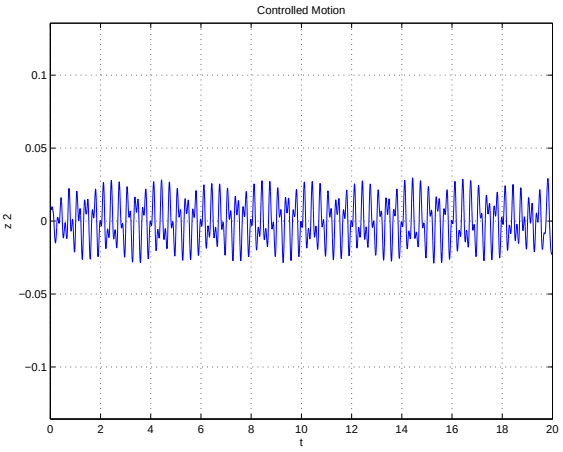

Figure 15: $x_2(t)$ - Controlled Motion - Case Study 2

absorber in the case of the uncontrolled motion is represented in figure 16 whereas the displacement of the absorber in the case of the controlled motion is represented in figure 17. The velocities of system floors and of the absorber in the case of the controlled motion exhibit an amplitude reduction qualitatively similar to that of their respective displacements. The iterative decrease of the cost function is represented in figure 18. The resulting controller is represented in figure 19. As can be seen from the preceding figures, the introduction of the controller drastically reduces the magnitudes of system displacements and velocities. This reduction can be

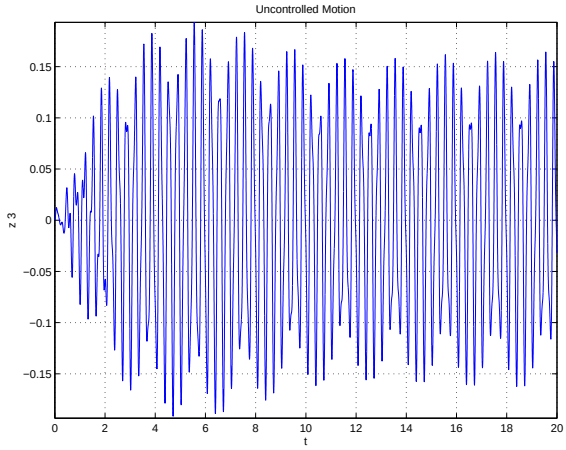

Figure 16: $x_3(t)$ - Uncontrolled Motion - Case Study 2

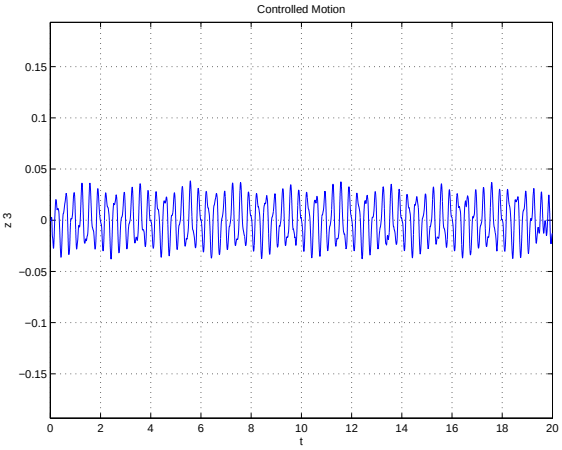

Figure 17: $x_3(t)$ - Controlled Motion - Case Study 2

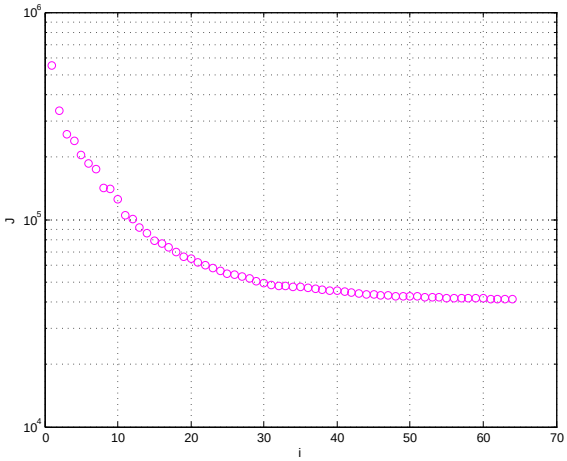

Figure 18: J_c - Performance Index - Case Study 2

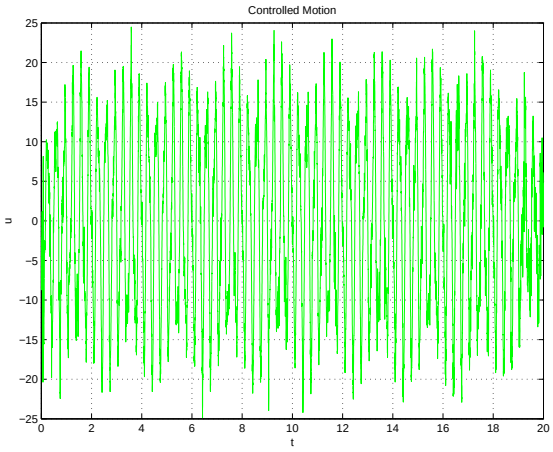

Figure 19: $u(t)$ - Control Action - Case Study 2

quantified comparing the maximum amplitudes of system motion with and without the controller. Indeed:

$$\varepsilon_{r,x_i} = \frac{\max\limits_{t\in[0,T]}(\mathrm{abs}(x_{i,uncontrolled}(t))) - \max\limits_{t\in[0,T]}(\mathrm{abs}(x_{i,controlled}(t)))}{\max\limits_{t\in[0,T]}(\mathrm{abs}(x_{i,uncontrolled}(t)))} = \begin{cases} 0.6979 \\ 0.7824 \\ 0.8014 \end{cases} \tag{34}$$

$$\varepsilon_{r,\dot{x}_i} = \frac{\max\limits_{t\in[0,T]}(\mathrm{abs}(\dot{x}_{i,uncontrolled}(t))) - \max\limits_{t\in[0,T]}(\mathrm{abs}(\dot{x}_{i,controlled}(t)))}{\max\limits_{t\in[0,T]}(\mathrm{abs}(\dot{x}_{i,uncontrolled}(t)))} = \begin{cases} 0.7375 \\ 0.6989 \\ 0.7600 \end{cases} \tag{35}$$

The magnitude reductions of floors and absorber displacements are greater than the 69% whereas the magnitude reductions of floors and absorber velocities are greater than the 69%.

5 CONCLUSIONS

In this paper authors propose the development of an efficient control method for nonlinear mechanical systems. The system analysed is a two-storey building model coupled with an active vibration absorber. The active vibration absorber considered is a hybrid mass damper subjected to a dry friction force. The control actuator is located between the second floor and the mass damper. Two approximated model for the dry friction force has been considered in order to facilitate the numerical integration procedure. For each friction model the control law has been obtained using optimal control theory and has been computed solving a constrained minimization problem by using an iterative adjoint-based optimization method. The effectiveness of the proposed algorithm has been tested in the worst-case scenario in which the system is excited by a ground motion whose harmonic content is close to the first two system natural frequencies. From the simulation results it is clear that the designed controller drastically reduces the amplitude of displacements and velocities relative to each system floor even in the considered worst-case scenario.

DESCRIPTION	SYMBOL	DATA [UNITS]
Length of Structural Element 1	L_1	$23 \cdot 10^{-2}[m]$
Length of Structural Element 2	L_2	$28 \cdot 10^{-2}[m]$
Second Moment of Area of Structural Element 1	J_1	$2.92 \cdot 10^{-12}[m^4]$
Second Moment of Area of Structural Element 2	J_2	$2.92 \cdot 10^{-12}[m^4]$
Mass of Floor 1	m_1	$1.3[kg]$
Mass of Floor 2	m_2	$0.8[kg]$
Mass of Absorber	m_3	$0.2[kg]$
Elastic Modulus of Structural Element 1	E_1	$207 \cdot 10^9[kg \cdot m^{-1} \cdot s^{-2}]$
Elastic Modulus of Structural Element 2	E_2	$207 \cdot 10^9[kg \cdot m^{-1} \cdot s^{-2}]$
Equivalent Stiffness of Structural Element 1	k_1	$1.19 \cdot 10^3[kg \cdot s^{-2}]$
Equivalent Stiffness of Structural Element 2	k_2	$660[kg \cdot s^{-2}]$
Stiffness of Absorber	k_3	$400[kg \cdot s^{-2}]$
Proportional Damping Coefficient of Mass Matrix	α	$1[s]$
Proportional Damping Coefficient of Stiffness Matrix	β	$3 \cdot 10^{-4}[s^{-1}]$
Ground Motion Amplitude 1	W_1	$5 \cdot 10^{-3}[m]$
Ground Motion Amplitude 2	W_2	$5 \cdot 10^{-3}[m]$
Ground Motion Frequency 1	f_1	$3[s^{-1}]$
Ground Motion Frequency 2	f_2	$6.5[s^{-1}]$
Dry Friction Coefficient	μ_0	$0.3[\backslash]$
Friction Model 1 Coefficient 1	D_1	$1[\backslash]$
Friction Model 1 Coefficient 2	D_2	$10[m^{-1} \cdot s]$
Friction Model 2 Coefficient 1	C_1	$40[kg \cdot s^{-1}]$
Friction Model 2 Coefficient 2	C_2	$1[\backslash]$
Friction Model 2 Coefficient 3	C_3	$400[kg^{-2}s^2]$
Friction Model 2 Coefficient 4	C_4	$0.25[kg \cdot s^{-1}]$
Initial Displacement of Floor 1	$x_{1,0}$	$1 \cdot 10^{-2}[m]$
Initial Displacement of Floor 2	$x_{2,0}$	$1 \cdot 10^{-2}[m]$
Initial Displacement of Absorber	$x_{3,0}$	$0[m]$
Initial Velocity of Floor 1	$v_{1,0}$	$0[m \cdot s^{-1}]$
Initial Velocity of Floor 2	$v_{2,0}$	$0[m \cdot s^{-1}]$
Initial Velocity of Absorber	$v_{3,0}$	$0[m \cdot s^{-1}]$
Time Span	T	$20[s]$
Time Step	Δt	$10^{-3}[s]$

Table 1: System Data

REFERENCES

[1] B. G. Korenev, L. M. Reznikov, Dynamic Vibration Absorbers: Theory and Technical Applications. *John Wiley and Sons*, ISBN: 047192850X.

[2] A. V. Srinivasan, D. M. McFarland, Smart Structures: Analysis and Design. *Cambridge University Press*, ISBN: 0521659779.

[3] D. J. Ewins, S. S. Rao, S. G. Braun, Encyclopedia of Vibration. *Academic Press*, ISBN: 0122270851.

[4] A. Hartung, H. Schmieg, P. Vielsack, Passive Vibration Absorber with Dry Friction. *Archive of Applied Mechanics*, Volume: 71, Issue: 6-7, July 2001, pp. 463 - 472.

[5] F. Nilvetti, C. M. Pappalardo, Experimental Investigation of a Virtual Passive Absorber For Structural Vibration Control. *International Journal of Mechanical Engineering and Industrial Design (JMEID)*, ISSN: 2280-6407, volume 1, 2012, 1(5): 83-90.

[6] D. Guida, F. Nilvetti, C. M. Pappalardo, Experimental Investigation of an Active Structural Control Device. *International Journal of Mechanical Engineering and Industrial Design (JMEID)*, ISSN: 2280-6407, Volume 1, 2012, 1(6): 91-96.

[7] D. Guida, F. Nilvetti, C. M. Pappalardo, Modelling, Identification and Control of a Three-Story Building System. *International Journal of Mechanical Engineering and Industrial Design (JMEID)*, ISSN: 2280-6407, Volume 1, 2012, 1(3): 36-60.

[8] D. Guida, F. Nilvetti, C. M. Pappalardo, Dry Friction Influence on Cart Pendulum Dynamics. *International Journal of Mechanics*, ISSN: 1998-4448, Issue 2, Volume 3, 2009, Pages 31-38.

[9] A. E. Bryson, Y. C. Ho, Applied Optimal Control: Optimization, Estimation and Control. *Taylor and Francis*, ISBN: 0891162283

[10] T. R. Bewley, Numerical Renaissance: Simulation, Optimization and Control. *Renaissance Press*, To be published.

[11] T. R. Bewley, A Linear Systems Approach to Flow Control. *Annual Review of Fluid Mechanics*, 39:383417, 2007.

[12] W. H. Press, S. A. Teukolsky, W. T. Vetterling, B. P. Flannery, Numerical Recipes: The Art of Scientific Computing. *Cambridge University Press*, ISBN: 0521880688